Sex differences exist in adult heart group 2 innate lymphoid cells

Hongyan Peng
Hunan Children's Hospital
Shuting Wu
Hunan Children's Hospital
Shanshan Wang
Sun Yat-sen University
Qinglan Yang
Hunan Children's Hospital
Lili Wang
Hunan Children's Hospital
Shuju Zhang
Hunan Children's Hospital
Minghui Huang
Hunan Children's Hospital
Yana Li
Hunan Children's Hospital
Peiwen Xiong
Hunan Children's Hospital
Zhaohui Zhang
Army Medical University (Third Military Medical University)
Yue Cai
Xijing Hospital, Fourth Military Medical University
Liping Li
Hunan Children's Hospital
Yafei Deng
Hunan Children's Hospital
Youcai Deng (youcai.deng@tmmu.edu.cn)
Army Medical University (Third Military Medical University)

Research Article

Keywords: Group 2 innate lymphoid cells (ILC2s), heart, sex difference, Klrg1, IL-33

Posted Date: June 22nd, 2022

DOI: https://doi.org/10.21203/rs.3.rs-1765137/v1

Abstract

Background: Group 2 innate lymphoid cells (ILC2s) are the most dominant ILCs in heart tissue, sex-related differences exist in mouse lung ILC2 phenotypes and functions; however, it is still unclear whether there are sex differences in heart ILC2s.

Results: Compared with age-matched wild-type (WT) male mice, 8-week-old but not 3 week-old WT female mice harbored an obviously greater percentage and number of heart ILC2s in homeostasis present. However, the percentage of killer-cell lectin-like receptor G1 $(Klrg1)^-$ ILC2s were higher but the $Klrg1^+$ ILC2s were lower in female mice than in male mice in both the heart tissue of 3- and 8-week-old mice. Eight-week-old *Rag2*$^{-/-}$ mice also showed sex differences similar to those of age-matched WT mice. Regarding surface marker expression, compared to age-matched male mice, WT female mice showed higher expression of CD90.2, and lower expression of Klrg1 and Sca-1 in heart total ILC2s. No sex difference in IL-4 and IL-5 secretion by male and female mice heart ILC2s. Increased *IL-33* mRNA levels within the heart tissues were also found in female mice compared with male mice.

Conclusions: These results have revealed the greater numbers of ILC2s, higher expression of CD90.2, reduced Klrg1 and Sca-1 expression in the heart of female mice than male mice and no sex difference in IL-4 and IL-5 production in male and female mice heart ILC2s. These sex differences of heart ILC2s might be due to the heterogeneity of IL-33 within the heart tissue.

Background

Group 2 innate lymphoid cells (ILC2s) are rare but potent ILCs that are involved in allergies and infections by mediating a type 2 immune response [1, 2]. ILC2s are characterized by the expression of the transcription factor Gata3 and the surface markers CD127 (IL-17R), CD90.2 (Thy1.2), and ST2 (IL-33R) ($Lin^-CD127^+CD90.2^+ST2^+$). They can produce type 2 cytokines, including interleukin (IL)-4, IL-5, and IL-13 [1, 2]. Our previous study and others have reported that ILC2s are the most dominant population of ILCs in the heart; this population is identified as $CD45^+$ $Lin^-CD127^+CD90.2^+ST2^+$cells [3, 4]. We found that heart-resident ILC2s have a unique phenotype characterized by lower expression of Icos, CD25 (IL-2Rα), and Ki-67 but higher expression of Stem cell antigen 1 (Sca-1) and Gata3 and a stronger ability to produce interleukin (IL)-4 and IL-13 than lung ILC2s [3].

Growing evidence manifest that sex difference exist in innate and adaptive immune cell, for instance, males have higher NK cell frequencies in peripheral blood[5], and female mice have higher level of $CD8^+$T cells and lower lever of regulatory T cells (Tregs) in adipose tissue [6]. Moreover, recent studies have revealed sex-related differences in mouse lung ILC2 phenotypes and functions, which also show strain differences [7]. Heart ILC2s, as dominat population of ILCs in heart, have been reported to play a protective role in mouse model of atherosclerosis [8] and contribute to IL-33-mediated protection of cardiac fibrosis in the mouse model of catecholamine-induced cardiac fibrosis [9]. However, it is still unclear whether there are sex differences in heart ILC2s.

To understand the sex differences in heart ILC2s, we investigated the number, phenotypes, and functions of heart ILC2s in both male and female mice at homeostasis. Here, we showed that male and female mice showed significant differences in the ratio and number of total ILC2s, as well as the Klrg1$^+$ and Klrg1$^-$ ILC2 subsets, in the heart at 8 weeks old. Compared with those of male mice, female mouse heart ILC2s exhibited higher expression of CD90.2 and Ki67; lower expression of Klrg1 and Sca-1, however, no difference in IL-4 and IL-5 production in male and female mice heart ILC2s. Furthermore, female 8-week-old *Rag2*-deficient (*Rag2*$^{-/-}$) mouse heart ILC2s and the Klrg1$^+$ and Klrg1$^-$ ILC2 subsets exhibited trends similar to those in WT mice. We also found that the increased *IL-33* mRNA levels existed within the heart tissues of female mice compared with male mice, which might be response for the sex difference of heart ILC2 frequencies and Klrg1 expression .

Results

Female mice show higher ratios and greater numbers of ILC2s in adult heart tissue

To investigate the differences in heart ILC2s between male and female mice, we collected Percoll-enriched heart lymphocytes from 3- and 8-week-old male and female mouse hearts. The gating strategy for heart ILC2s is shown in **Fig.1A**. At 3 weeks of age, the ratio and number of heart ILC2s were indistinguishable between male and female mice (**Fig.1B**). At 8 weeks of age, both the ratio and the total number of heart ILC2s were higher in female mice than in age-matched male mice hearts (**Fig.1C**).

Based on Klrg1 expression, a recent study reported that the numbers of Klrg1$^-$ ILC2s in the bone marrow and lungs are downregulated by androgen [10]. Therefore, we further investigated the sex differences in Klrg1$^-$ and Klrg1$^+$ ILC2s. The ratio and numbers of heart Klrg1$^-$ ILC2 ratio were higher in female mice than in male mice at the age of both 3 and 8 weeks of age when CD45$^+$Lin$^-$CD127$^+$CD90.2$^+$ST2$^+$ ILC2s were assessed. As for the heart Klrg1$^+$ ILC2s, the ratio was decreased but the numbers showed increased at 8-week- old mice, but the decreased ratio and the decreasing trend of the number of the heart Klrg1$^+$ ILC2s have been found at 3-week-old (**Fig.1D-1E**).

Besides, we also measured the protein levels of Gata3 in heart ILC2s, and found that both male and female mice heart ILC2 gated by CD45$^+$Lin$^-$CD127$^+$CD90.2$^+$ST2$^+$ almost all are Gata3$^+$ cells. The ratio among CD45$^+$ cells and the numbers of Gata3$^+$ ILC2s were higher in female mice than male mice (**Fig.S1A**). To further illustrate heart ILC2s exist sex difference, we gated CD45$^+$Lin$^-$ CD90.2$^+$CD127$^+$ Gata3$^+$ for ILC2, and we found that the ratio of ILC2s among CD45$^+$ cells were higher in female mice than male mice (**Fig.S1B**). The above data suggest that sex hormones may play an extrinsic role in determining the number of heart ILC2s, especially the numbers of Klrg1$^-$ ILC2s and Klrg1$^+$ ILC2s in the heart.

Phenotypic differences in heart ILC2s between male and female mice

We next investigated the sex differences in murine heart ILC2 phenotypes, including surface markers, transcription factors, and proliferation. In total heart ILC2s, the geometric mean fluorescence intensity (gMFI) of Klrg1 and Sca-1 was lower, while CD90.2 (Thy1.2) were higher in 8-week-old female mice than in age-matched male mice (**Fig.2A**). There were no sex differences in the gMFIs of other surface markers, including Icos, CD25 (IL-2Rα), CD127 (IL-17R) and ST2 (IL-33R), or in that of the transcription factor Gata3 (**Fig.2A**). In addition, female mice heart ILC2s had a stronger proliferation ability than male mice, which was reflected by increased the Ki-67$^+$ cells (**Fig.2B**). These results demonstrated that mouse heart total ILC2s had distinct sex differences in terms of the surface expression of Klrg1, Sca-1, CD90.2 and proliferation ability.

Because our results showed that the numbers of Klrg1$^-$ ILC2s and Klrg1$^+$ ILC2s in the heart exhibited sex differences, we next determined the sex differences in heart Klrg1$^-$ or Klrg1$^+$ ILC2 phenotypes. Our results showed that the gMFI of CD90.2 was increased, and the gMFI of Sca-1 was decreased in both Klrg1$^-$ and Klrg1$^+$ ILC2s in the heart of female mice, but the gMFI of Klrg1 was also decreased in Klrg1$^+$ ILC2s in female mice heart (**Fig.2A**). The Ki67-positive cells were higher in both Klrg1$^-$ ILC2s and Klrg1$^+$ ILC2s in female mice hearts (**Fig.2B**). There were no sex differences in CD25, Icos or Gata3 among heart Klrg1$^-$ ILC2s and Klrg1$^+$ ILC2s (**Fig.2A**).

Cytokines secreted by heart ILC2s in male and female mice

ILC2s are known to produce the main type 2 cytokines, IL-4 and IL-5, after stimulation with IL-25, IL-33 and TSLP. To investigate the expression of these cytokines in male and female mouse heart ILC2s, we stimulated heart lymphocytes with 50 ng/ml IL-33 for 4 hours and then determined the production of IL-4 and IL-5 by the ILC2s through flow cytometry. Our results showed that heart ILC2 showed lower ratio of IL-4 in female mice than in age-matched male mice (**Fig.3A**), but the total number of IL-4$^+$ ILC2 and the gMFI of IL-4 exhibited no significance difference between male and female mice heart ILC2s (**Fig.3A**). There was no significant difference of IL-5 production, regarding the ratio, total number and gMFI, in heart ILC2s between male and female mice (**Fig.3B**).The above data suggest that IL-4 and IL-5 secreted by heart ILC2s are not affected by sex hormone.

The number and ratio of heart ILC2s are different between male and female *Rag2*$^{-/-}$ mice

ILC2s are thought to be regulated by regulatory T (Treg) cells that also express IL-33R (also named ST-2) [11, 12], and sex hormones are known to affect Treg cells [6]. As such, we also determined the ratio and number of heart ILC2s in male and female *Rag2*$^{-/-}$ mice, which lack functional T and B cells, at the age of 8 weeks old. The data showed a higher ratio and number of total heart ILC2s in female mice than in male mice (**Fig.4A**). The ratios and numbers of heart Klrg1$^-$ and Klrg1$^+$ ILC2s between male and female *Rag2*$^{-/-}$ mice showed trends similar to those observed for WT mice (**Fig.4B**). Interestingly, the number of total heart ILC2s in *Rag2*$^{-/-}$ mice was almost 3-fold higher than that in WT mice (male mice: 258.89 ± 157.84 *vs.* 1000.6 ± 220.18; female mice: 570.11 ± 310.08 *vs.* 1612.00 ± 321.78). The increased number of heart

ILC2s in *Rag2*$^{-/-}$ mice was mainly contributed by Klrg1^{-} ILC2s. This difference might be attributed to Treg cells, partly because Treg cells repress ILC2 functions directly or compete for IL-33 in heart tissue [11].

Because our results showed that the phenotype of heart ILC2s and Klrg1^{-} ILC2s and Klrg1^{+} ILC2s, including Klrg1 and CD90.2, was different in male and female WT mice, we also determined the sex difference of heart Klrg1^{-} or Klrg1^{+} ILC2s in phenotypes. Our results showed that the gMFI levels of Klrg1 were lower but CD90.2 was higher in female *Rag2*$^{-/-}$ mice (**Fig.4C**), which was similar in WT mice. Moreover, the gMFI levels of CD90.2 were increased but the gMFI levels of Klrg1 were decreased in both subsets, but the gMFI of CD127 was higher in only female mouse heart Klrg1^{-} ILC2s (**Fig.4C**). There was no sex difference of ST2 among heart Klrg1^{-} ILC2s and Klrg1^{+} ILC2s (**Fig.4C**).

Expression of hormone receptors on heart ILC2s and IL-33 in the heart tissue

We further explore whether the sex differences of heart ILC2s is dependent on cell intrinsic sex hormone receptor expression levels or extrinsic cytokines from heart local tissues. Previous studies have found that Lung ILC2s showed higher expression levels of androgen receptor (Ar) and lower expression of estrogen receptor 1 (Esr1) and not expression of Esr2 [13], and sex hormones, such as androgen play an extrinsic role in determining the numbers of lung ILC2s and also ILC2 progenitors [14, 15]. To this end, we measured the mRNA expression of *Ar*, *Esr1* and *Esr2* in both male and female mice heart ILC2s, and found that the mRNA levels of *Ar*, *Esr1* and *Esr2* were undetectable in both male and female mice heart ILC2s (**Fig.5A**). Consistently, the ratios and surface marker expression of heart ILC2s from both male and female mice were not changed after different concentrations of 17β-E2 (estrogen) or testosterone (androgen) stimulation for 4 hours (**Fig.S2A-S2D**).

To further explore the extrinsic factors, such as cytokines, that response for the sex difference of heart ILC2s, we determined the mRNA levels of *IL-33*, which is reported to maintain ILC2 homeostasis and expansion in the heart tissues of both male and female mice at homeostatic state [16-18]. The data revealed relative higher mRNA levels of IL-33 in female mice heart tissue than male mice (**Fig.5B**). Collectively, these data suggested that the sex difference of heart ILC2s is not dependent on sex hormone receptor expression but might be associated with the higher levels of IL-33 within the heart tissue of female mice.

Single-cell transcriptional profiles of heart ILC2s in male and female mice

To further explore the sex difference of heart ILC2s at the single-cell level, we reanalyzed the single-cell RNA sequencing (scRNA-seq) data that contained six male and four female mice heart samples from published datasets [19, 20]. After initial quality control checks, we identified 8 main clusters among mouse heart lymphocytes based on marker gene expressions across all cells by uniform manifold approximation and projection (UMAP) analysis (Figure.S3A). Cell plots with red circles were attributed to ILC2s, which was confirmed by the high expression of *Gata3* and *Il17r* (**Fig.S3A-S3B**). Because these samples of scRNA-seq were mixtures of cells derived from both male and female mice, we isolated male

and female lymphocytes based on expression of female specific gene *Xist* (X-inactive specific transcript) [19] (**Fig.S3C**). The data showed relative higher ratios of ILC2s in female mice than male mice (**Fig.6A**), which is consistent with our flow cytometric results. We identified 59 differential genes expression in heart ILC2s from male and female mice, such as subunit of activator protein-1 (AP-1), Fosb, and Fosl2 that were reported to be implicated in cell proliferation [21] (**Fig.6B**). Gene set variation analysis (GSVA) analysis revealed that the pathway of glycine, serine and threonine metabolism was unregulated, while other signaling pathways, such as B cell receptor signaling pathway, alpha-Linolenic acid metabolism, were downregulated in female heart ILC2s compared with male heart ILC2s (**Fig.6C**).

Discussion

Recent studies have highly demonstrated tissue- and even strain-specific sex differences in resident ILC2s [10, 14, 22]. The frequency and numbers of ILC2s were found to be higher in the visceral adipose tissue, mesenteric lymph nodes and lungs of adult female mice than in those of male mice under steady-state conditions [10, 14]. We and other groups have reported that ILC2s are the most dominant population of ILCs in the heart [3, 4]. In the current study, we found that the ratio and number of total ILC2s in the heart were significantly higher in female mice than male mice in adulthood but not at 3 weeks old in the steady state. In addition, female and male *Rag2*$^{-/-}$ mice showed similar trends for the ratio and numbers of total ILC2s and Klrg1 expression.

In female C57BL/6J mice, lung ILC2s exhibited increased expression of CD90.2 and decreased expression of Klrg1 [7, 10, 14]. Similarly, our current study showed that female mouse heart ILC2s exhibited higher expression levels of CD90.2 but lower expression of Klrg1 and Sca-1 at 8- weeks' old age. Klrg1 is expressed on ILC2s, natural killer (NK) cells and CD8^{+} T cells and is an inhibitory receptor that contains an immunoreceptor tyrosine-based inhibitory motif (ITIM) [23–25]. Recent reports have revealed Klrg1 interacts with E-cadherin in epithelial tissue to blunt mouse lung ILC2 proliferation [26, 27]. Consistent with this scenario, our data showed that female heart Klrg1^{+} ILC2s showed a reduced MFI for Klrg1 along with increased Ki-67 expression. Consistently, our scRNA-seq analysis showed that female mice heart ILC2s owned higher expression of Fosb and Fosl2, a subunit of activator protein-1 (AP-1) implicated in cell proliferation [21]; whereas male mice heart ILC2s showed upregulation of α-linolenic acid metabolism, which decreases T cell proliferation and differentiation [28].

Previous studies have demonstrated that sex differences of ILC2s are regulated by both sex hormone receptor dependent and independent pathways [13]. In our study, murine heart ILC2s expressed almost undetectable sex hormone receptors and heart ILC2s showed no sex differences in response to sex hormone stimulation, which suggests that the sex difference of murine heart ILC2s is not dependent on sex hormone. However, our results revealed a relative higher mRNA level of IL-33 in the heart tissue of female mice than male mice at a steady state. Previous studies have demonstrated that IL-33 enhances ILC2 ratios at steady state [16]. All these evidence suggest that the heterogeneity of IL-33 levels in the heart tissue may contribute to the increased ratio and Klrg1 expression of heart ILC2s in female mice at a steady state.

Conclusions

In summary, the results of the present study present the sex differences in adult murine heart ILC2s, characterized by female mice harboring obviously greater numbers of heart ILC2s in homeostasis, due to a major subset of Klrg1$^-$ ILC2s, and no sex difference in IL-4 and IL-5 production, which might because of the heterogeneity of IL-33 levels within the heart tissue.

Methods

Animals

Male and female WT C57BL/6 mice were maintained in the Hunan Children's Research Institute pathogen-free animal facility of Hunan Children's Hospital (Changsha, Hunan, China). Mice were housed in cages (4–5 mice maximum per cage) at 22–25°C and 50 ± 10% relative humidity with a 12-hour light/dark cycle, periodic air changes, and free access to water and food. Congenic *Rag2*$^{-/-}$ mice on the C57BL/6 background were obtained from Changzhou Cavens Laboratory Animal Co., Ltd. (Changzhou, Jiangsu, China). All animal procedures and protocols were approved by the Animal Ethics Committee of Hunan Children's Hospital and followed the guidelines of the Institutional Animal Care and Use Committees of Hunan Children's Hospital (Changsha, Hunan, China).

Single-cell suspension preparation

A single-cell suspension was prepared as described previously [3]. Mice were anesthetized with 2% pentobarbital sodium, and the heart was slowly perfused with cold phosphate-buffered saline (PBS) administered via the left ventricle with a 5-ml syringe to remove peripheral blood cells. Then, heart tissues were cut into approximately 1-cm^2 pieces and digested for 45 min at 37°C in Hank's solution containing 10% fetal bovine serum (FBS) (Biological Industry, Kibbutz Beit Haemek, Israel), 0.5 mg/ml collagenase I (Sigma-Aldrich, St. Louis, MO, United States), and 0.5 mg/ml collagenase II (Gibco, Waltham, MA, United States). After digestion, the cells were resuspended in 20% Percoll (GE Healthcare, Pittsburgh, PA, United States) in RPMI 1640 medium (Biological Industry, Kibbutz Beit Haemek, Israel) containing 5% FBS and collected after centrifugation (2000 rpm, room temperature, 5 min).

Antibodies and flow cytometry

The antibodies used for flow cytometry were commercially purchased and are listed in **Table 1.** For surface markers, single-cell suspensions derived from heart tissues were stained by incubating the cells with antibodies in staining buffer (PBS containing 2% mouse serum, 2% horse serum and anti-CD16/CD32 blocking antibodies (eBioscience, San Diego, CA, United States) for 15 min at room temperature in the dark). For life-dead staining, cells were incubated with 7-AAD in apoptosis staining buffer (BioLegend, San Diego, San Diego, CA, United States) for 15 min at 4°C after surface marker staining. Gata3 and Ki67 were stained as recommended by the manufacturer using the Foxp3/Transcription Factor Staining Buffer Set Kit (eBioscience, San Diego, CA, United States). The

lineage (Lin) markers included CD3ε and CD19. Isotype-matched control antibodies were used at the same concentration as the corresponding test antibody. All flow cytometry experiments were carried out on a BD LSRFortessa (BD Biosciences, San Diego, CA, United States). Data were analyzed with FlowJo software (version 10.0; FlowJo LLC, Ashland, OR United States).

RNA Isolation and qRT-PCR Analysis

Single-cell suspensions isolated from heart tissues were stimulated with DMSO or 50 ng/ml IL-33 for 4 hours and then were used for RNA extraction by Total RNA Purification Micro Kit (Norgen BioTek Corp, Thorold, ON, Canada). Total RNA was extracted from heart tissue using Trizol (Invitrogen, Waltham, MA, United States), as described previously [3]. Total RNA was then reverse transcribed into cDNA through *Evo M-MLV* RT Premix (AG Biotechnology (Hunan), Changsha, China). Real-time qPCR was performed using SYBR® Green Premix *Pro Tag* HS qPCR Kit (AG Biotechnology (Hunan), Changsha, China) with a Roche LightCycler® 480 II. Primer sequences used for qRT-PCR were obtained from reported literatures or designed by Pubmed Primer-BLAST. Primer sequences used for qRT-PCR were obtained designed by Pubmed Primer-BLAST, including: Ar forward, 5’-CAGGAGG TAATCTCCGAAGGC-3’; Ar reverse, 3’-ACAGACACTGCTTTACACAACTC-5’; Esr1 forward, 5’-CCCGCCTTCTACAGGTCTAAT-3’; Esr1 reverse, 3’-CTTTCTCGTTACTGCTGGACAG-5’; Esr2 forward, 5’-CTGTGATGAACTACAGTGTTCCC-3’; Esr2 reverse, 3’-CACATTTGGGCTTGCAGT CTG -5’; Primer sequences used for qRT-PCR were obtained from reported literatures, including IL-33 forward, 5’-CCCTGGTCCCGCCTTGCAAAA-3'; IL-33 reverse, 3’-AGTTCTCTTCATGCTTGGTA CCCGA-5’ [3]; GAPDH forward, 5’-AGGTCGGTGTGAACGGATTTG-3’; GAPDH reverse, 3’ TG TAGACCATGTAGTTGAGGTCA-5’.

Analysis of sex hormone response of heart ILC2s

For the analysis of heart ILC2s response to sex hormones, single-cell suspensions isolated from heart tissues were stimulated with 0, 0.1, 1 and 10 μM 17β-estradiol (17β-E2) and testosterone (Medchem Express, Monmouth Junction, NJ, United States) for 4 hours and then stained for surface markers. All flow cytometry experiments were carried out on a BD LSRFortessa. Data were analyzed with FlowJo software.

IL-4 and IL-5 production

For intracellular IL-5 and IL-4 staining, single-cell suspensions isolated from heart tissues were stimulated with 50 ng/ml IL-33 (BioLegend, San Diego, San Diego, CA, United States) plus BD Golgi Plug protein transport inhibitor (BD Biosciences, San Diego, CA, United States) for 4 hours and then stained for surface markers. After washing, the cells were fixed with the Fixation/Permeabilization Solution Kit (BD Biosciences, San Diego, CA, United States) following the manufacturer’s instructions and stained with anti-IL-4 or anti-IL-5 antibodies. Isotype-matched control antibodies were used at the same concentration as the corresponding test antibody. All flow cytometry experiments were carried out on a BD LSRFortessa. Data were analyzed with FlowJo software.

scRNA-seq analysis of heart ILC2s

Two datasets containing 10 female and male-mixed mouse heart samples (6 normal heart samples) were downloaded from ArrayExpress database [19, 20] for downstream analysis. Cell Ranger version (version 6.0.1) was used to process raw sequencing data. Seurat R package (version 4.0.5) was applied in our study to convert the scRNA-seq data as a Seurat object [29]. Cells that expressed fewer than 300 genes or more than 5000 genes, or had more than 20% mitochondrial genes, were removed at the quality control step. Data were then normalized by SCT transform R package (version 0.3.2) [30]. Next, we used the "RunPCA" function to reduce the dimension of the scRNA-seq data. Subsequently, we used the "RunPCA" function to conduct the UMAP analysis. We also used the "Find Clusters" and "Find All Markers" functions to conduct cell clustering analysis and detect gene expression markers. Afterwards, we used the Single R package and Cell Marker dataset to annotate the cell types in our study [31]. The "subset" function was also applied to extract the sub-cluster for downstream analysis and then annotated and analyzed as described above. Cells with Xist gene expression ≥ 0.1 was identified from female mice. To analyze the DEGs between female and male ILC2s, the value of logFC threshold was set to 0.25 to filter the DEGs, and the heatmap was produced by the Complex Heatmap R package (version 2.11.1). GSVA was used to assess KEGG pathway activation in the GSVA R package (version 1.42.0) [32].

Statistical analysis

All data are expressed as the mean ± SD, and statistical analyses were performed with SPSS software for Windows (Version 23, SPSS Inc., Chicago, IL, United States). Statistical analysis was performed with an unpaired Student's t-test for comparisons of two independent experimental groups. If the litter effect was very obvious among independent experiments, two-way ANOVA (sex and litter) followed by Dunnett's test was used [33]. In each analysis, there were n = 5–12 replicates per group, and the results are representative of at least two independent experiments. Statistical significance was defined as $P < 0.05$. The number of mice used in each group is indicated in the figure legends. All graphs were produced by GraphPad Prism 8.0 for Windows software (GraphPad Software Inc., La Jolla, CA, United States).

Abbreviations

CVDs: Cardiovascular diseases; ILC2: group 2 innate lymphoid cells; ILC: innate lymphoid cells; WT: wild-type; Klrg1: killer-cell lectin-like receptor G1; Sca-1: Stem cell antigen 1; IL: interleukin; gMFI: geometric mean fluorescence intensity; Ar: androgen receptor; Er: estrogen receptor; 17β-E2: 17β-estradiol; Xist: X-inactive specific transcript; scRNA-seq: single-cell RNA sequencing; UMAP: uniform manifold approximation and projection; DEGs: differentially expressed genes; GSVA: Gene set variation analysis.

Declarations

Ackonwledgements

Not applicable.

Author contributions

The work presented was performed in collaboration with all authors. HP designed and performed the experiments, analyzed the data, and wrote the manuscript. SWa, SWu, QY, LW, SZ, MH, YL, PX, ZZ, and YC performed the experiments and analyzed the data. LL designed the research and supervised the study. YaD designed the research and analyzed the data. YoD devised the concept, designed the research, supervised the study, and wrote the manuscript.

Funding

This study was supported by funding from the National Natural Science Foundation of China (No. 81900055 to HP; Nos. 81874313, 81922068 to YoD). This study was also supported by funding from the Natural Science Foundation of Hunan Province (No. 2021JJ40274 to HP). This work was also supported by funding from the Science Foundation of Hunan Children's Hospital (2019 and 2021).

Availability of data and materials

All data are included in the manuscript. The datasets analyzed in the current study are available from the corresponding author on reasonable request.

Ethics approval and consent to participate

All methods in this current study are reported in accordance with ARRIVE guidelines. The studies involving animal procedures and protocols were approved by the Animal Ethics Committee of Hunan Children’s Hospital, and the ethics committee approval code was HCHDWLL-2020-03. This study does not involve the use of human data or tissue. All experiments were performed in accordance with relevant guidelines and regulations at Hunan Children’s Hospital. All mice were sacrificed by cervical dislocation under anesthesia with 2% pentobarbital sodium.

Consent for publication

Not applicable.

Competing interests

The authors declare that they have no competing interests.

Authors’ information

Hongyan Peng [1,2,*], Shuting Wu [1,2,*], Shanshan Wang[3], Qinglan Yang [1,2], Lili Wang [1,2], Shuju Zhang [1,2], Minghui Huang [1,2], Yana Li [1,2], Peiwen Xiong [1,2], Zhaohui Zhang [4], Yue Cai [5], Liping Li [1,2], Yafei Deng [1,2,#], Youcai Deng [4,#]

Author details

[1]Pediatrics Research Institute of Hunan Province, Hunan Children’s Hospital, Changsha 410007, China;

[2]Hunan Provincial Key Laboratory of Children's Emergency Medicine, Hunan Children's Hospital, Changsha 410007, China;

[3]State Key Laboratory of Ophthalmology, Zhongshan Ophthalmic Center, Sun Yat-sen University, Guangzhou 510060, P. R. China;

[4]Institute of Materia Medica, College of Pharmacy, Army Medical University (Third Military Medical University), Chongqing 400038, China;

[5]Department of Cardiology, Xijing Hospital, Fourth Military Medical University, Xi’an 710032, China

References

1. Stehle C, Hernandez DC, Romagnani C. Innate lymphoid cells in lung infection and immunity. Immunol Rev. 2018; doi: 10.1111/imr.12712
2. Vivier E, Artis D, Colonna M, Diefenbach A, Di Santo JP, Eberl Get al. Innate Lymphoid Cells: 10 Years On. Cell. 2018; doi: 10.1016/j.cell.2018.07.017
3. Deng Y, Wu S, Yang Y, Meng M, Chen X, Chen Set al. Unique Phenotypes of Heart Resident Type 2 Innate Lymphoid Cells. Front Immunol. 2020; doi: 10.3389/fimmu.2020.00802
4. Bracamonte-Baran W, Chen G, Hou X, Talor MV, Choi HS, Davogustto Get al. Non-cytotoxic Cardiac Innate Lymphoid Cells Are a Resident and Quiescent Type 2-Commited Population. Front Immunol. 2019; doi: 10.3389/fimmu.2019.00634
5. Abdullah M, Chai PS, Chong MY, Tohit ER, Ramasamy R, Pei CPet al. Gender effect on in vitro lymphocyte subset levels of healthy individuals. Cell Immunol. 2012; doi: 10.1016/j.cellimm.2011.10.009
6. Ahnstedt H, Roy-O'Reilly M, Spychala MS, Mobley AS, Bravo-Alegria J, Chauhan Aet al. Sex Differences in Adipose Tissue CD8(+) T Cells and Regulatory T Cells in Middle-Aged Mice. Front Immunol. 2018; doi: 10.3389/fimmu.2018.00659
7. Loering S, Cameron GJ, Bhatt NP, Belz GT, Foster PS, Hansbro PMet al. Differences in pulmonary group 2 innate lymphoid cells are dependent on mouse age, sex and strain. Immunol Cell Biol. 2021; doi: 10.1111/imcb.12430
8. Newland SA, Mohanta S, Clement M, Taleb S, Walker JA, Nus Met al. Type-2 innate lymphoid cells control the development of atherosclerosis in mice. Nat Commun. 2017; doi: 10.1038/ncomms15781
9. Kabata H MK, Koyasu S. The group 2 innate lymphoid cell (ILC2) regulatory network and its underlying mechanisms. Immunol Rev. 2018; doi: 10.1111/imr.12706

10. Kadel S, Ainsua-Enrich E, Hatipoglu I, Turner S, Singh S, Khan Set al. A Major Population of Functional KLRG1(-) ILC2s in Female Lungs Contributes to a Sex Bias in ILC2 Numbers. Immunohorizons. 2018; doi: 10.4049/immunohorizons.1800008
11. Rigas D, Lewis G, Aron JL, Wang B, Banie H, Sankaranarayanan Iet al. Type 2 innate lymphoid cell suppression by regulatory T cells attenuates airway hyperreactivity and requires inducible T-cell costimulator-inducible T-cell costimulator ligand interaction. J Allergy Clin Immunol. 2017; doi: 10.1016/j.jaci.2016.08.034
12. Molofsky AB, Van Gool F, Liang HE, Van Dyken SJ, Nussbaum JC, Lee Jet al. Interleukin-33 and Interferon-gamma Counter-Regulate Group 2 Innate Lymphoid Cell Activation during Immune Perturbation. Immunity. 2015; doi: 10.1016/j.immuni.2015.05.019
13. Blanquart E, Laffont S, Guery JC. Sex hormone regulation of innate lymphoid cells. Biomed J. 2021; doi: 10.1016/j.bj.2020.11.007
14. Laffont S, Blanquart E, Savignac M, Cenac C, Laverny G, Metzger Det al. Androgen signaling negatively controls group 2 innate lymphoid cells. J Exp Med. 2017; doi: 10.1084/jem.20161807
15. Blanquart E, Mandonnet A, Mars M, Cenac C, Anesi N, Mercier Pet al. Targeting androgen signaling in ILC2s protects from IL-33-driven lung inflammation, independently of KLRG1. J Allergy Clin Immunol. 2021; doi: 10.1016/j.jaci.2021.04.029
16. Bartemes KR, Iijima K, Kobayashi T, Kephart GM, McKenzie AN, Kita H. IL-33-responsive lineage-CD25 + CD44(hi) lymphoid cells mediate innate type 2 immunity and allergic inflammation in the lungs. J Immunol. 2012; doi: 10.4049/jimmunol.1102832
17. Chen WY, Wu YH, Tsai TH, Li RF, Lai AC, Li LCet al. Group 2 innate lymphoid cells contribute to IL-33-mediated alleviation of cardiac fibrosis. Theranostics. 2021; doi: 10.7150/thno.51648
18. De Salvo C, Buela KA, Creyns B, Corridoni D, Rana N, Wargo HLet al. NOD2 drives early IL-33-dependent expansion of group 2 innate lymphoid cells during Crohn's disease-like ileitis. J Clin Invest. 2021; doi: 10.1172/JCI140624
19. McLellan MA, Skelly DA, Dona MSI, Squiers GT, Farrugia GE, Gaynor TLet al. High-Resolution Transcriptomic Profiling of the Heart During Chronic Stress Reveals Cellular Drivers of Cardiac Fibrosis and Hypertrophy. Circulation. 2020; doi: 10.1161/CIRCULATIONAHA.119.045115
20. Skelly DA, Squiers GT, McLellan MA, Bolisetty MT, Robson P, Rosenthal NAet al. Single-Cell Transcriptional Profiling Reveals Cellular Diversity and Intercommunication in the Mouse Heart. Cell Rep. 2018; doi: 10.1016/j.celrep.2017.12.072
21. Barrett CS, Millena AC, Khan SA. TGF-beta Effects on Prostate Cancer Cell Migration and Invasion Require FosB. Prostate. 2017; doi: 10.1002/pros.23250
22. Matha L, Shim H, Steer CA, Yin YH, Martinez-Gonzalez I, Takei F. Female and male mouse lung group 2 innate lymphoid cells differ in gene expression profiles and cytokine production. PLoS One. 2019; doi: 10.1371/journal.pone.0214286
23. Hoyler T, Klose CS, Souabni A, Turqueti-Neves A, Pfeifer D, Rawlins ELet al. The transcription factor GATA-3 controls cell fate and maintenance of type 2 innate lymphoid cells. Immunity. 2012; doi:

10.1016/j.immuni.2012.06.020

24. Tessmer MS, Fugere C, Stevenaert F, Naidenko OV, Chong HJ, Leclercq Get al. KLRG1 binds cadherins and preferentially associates with SHIP-1. Int Immunol. 2007; doi: 10.1093/intimm/dxm004
25. Henson SM, Franzese O, Macaulay R, Libri V, Azevedo RI, Kiani-Alikhan Set al. KLRG1 signaling induces defective Akt (ser473) phosphorylation and proliferative dysfunction of highly differentiated CD8 + T cells. Blood. 2009; doi: 10.1182/blood-2009-01-199588
26. Li Y, Hofmann M, Wang Q, Teng L, Chlewicki LK, Pircher Het al. Structure of natural killer cell receptor KLRG1 bound to E-cadherin reveals basis for MHC-independent missing self recognition. Immunity. 2009; doi: 10.1016/j.immuni.2009.04.019
27. Salimi M, Barlow JL, Saunders SP, Xue L, Gutowska-Owsiak D, Wang Xet al. A role for IL-25 and IL-33-driven type-2 innate lymphoid cells in atopic dermatitis. J Exp Med. 2013; doi: 10.1084/jem.20130351
28. Winnik S, Lohmann C, Richter EK, Schafer N, Song WL, Leiber Fet al. Dietary alpha-linolenic acid diminishes experimental atherogenesis and restricts T cell-driven inflammation. Eur Heart J. 2011; doi: 10.1093/eurheartj/ehq501
29. Macosko EZ, Basu A, Satija R, Nemesh J, Shekhar K, Goldman Met al. Highly Parallel Genome-wide Expression Profiling of Individual Cells Using Nanoliter Droplets. Cell. 2015; doi: 10.1016/j.cell.2015.05.002
30. Hafemeister C, Satija R. Normalization and variance stabilization of single-cell RNA-seq data using regularized negative binomial regression. Genome Biol. 2019; doi: 10.1186/s13059-019-1874-1
31. Aran D, Looney AP, Liu L, Wu E, Fong V, Hsu Aet al. Reference-based analysis of lung single-cell sequencing reveals a transitional profibrotic macrophage. Nat Immunol. 2019; doi: 10.1038/s41590-018-0276-y
32. Hänzelmann S CR, Guinney J. GSVA_ gene set variation analysis for microarray and RNA-seq data. BMC Bioinformatics. 2013; doi: 10.1186/1471-2105-14-7
33. MF F. Design and statistical methods in studies using animal models of development. ILAR J. 2006; doi: doi: 10.1093/ilar.47.1.5

Tables

Table 1 Antibodies used for flow cytometry

Antibodies	Clone	Source	Dilution
Anti-mouse CD45	30-F11	BioLegend	1/200
Anti-mouse CD3ε	145-2C11	BioLegend	1/200
Anti-mouse CD19	6D5	BioLegend	1/200
Anti-mouse CD127	SB/199	BD Bioscience	1/100
Anti-mouse CD90.2	53-2.1	BioLegend	1/100
Anti-mouse ST2	U29-93	BD Bioscience	1/100
Anti-mouse Klrg1	2F1	BioLegend	1/100
Anti-mouse ICOS	7E.17G9	BioLegend	1/100
Anti-mouse CD25	UC10-4B9	BioLegend	1/100
Anti-mouse Sca-1	D7	BioLegend	1/100
Anti-mouse Gata3	16E10A23	BioLegend	1/20
Anti-mouse IgG2b	MPC-11	BioLegend	1/100
Anti-mouse Ki67	SolA15	Thermo-eBioscience	1/100
Anti-mouse IgG2a	eBR2a	Thermo-eBioscience	1/100
Anti-mouse IL-4	11B11	BD Bioscience	1/50
Anti-mouse IgG1	R3-34	BD Bioscience	1/50
Anti-mouse IL-5	TRFK5	Thermo-Invitrogen	1/50
Anti-mouse IgG1	eBRG1	Thermo-Invitrogen	1/50
Anti-mouse TGF-β R2		R&D system	1/20
Anti-goat IgG		R&D system	1/20

Figures

Figure 1

The ratio and numbers of ILC2 in C57/B6L mouse heart tissue in 3- or 8- weeks old wild type mice. **A** Gate strategy of heart ILC2s in mice. Lineage (Lin) markers included CD3e, CD19. The number inside of gate indicates cell events. **B-C** Cumulative frequencies and enumeration of heart ILC2s among $CD45^{+}$ lymphocyte in 3-week-old (**B**) and 8-week-old (**C**) wild type mice by flow cytometric analysis. **D-E**

Cumulative frequencies and enumeration of KLRG1$^-$ILC2s and KLRG1$^+$ ILC2s among heart ILC2s in 3 weeks (**D**) and 8 weeks (**E**) wild type mice by flow cytometric analysis. Each dot represents one mouse; different color represents different litter; error bars represent mean ± SD; *p < 0.05, **p < 0.01, ***p < 0.001. Two-way ANOVA followed by Dunnett's test (B-E).

Figure 2

Phenotype difference between male and female mice heart ILC2s. **A** The geometric mean fluorescence intensity (gMFI) of indicated surface makers in heart ILC2s (identification as CD45$^+$Lin$^-$CD127$^+$CD90.2$^+$ ST2$^+$cells) and heart KLRG1$^-$ILC2s and KLRG1$^+$ ILC2s of 8 weeks old mice. **B** The cumulative frequencies of Ki67 expression in heart ILC2s and KLRG1$^-$ILC2s and KLRG1$^+$ ILC2s of 8 weeks old mice by flow cytometric analysis. Each dot represents one mouse; different color represents different litter; error bars represent mean ± SD; *p < 0.05, **p < 0.01. Two-way ANOVA followed by Dunnett's test (A-B).

Figure 3

Cytokine production ability for heart ILC2s in 8 weeks old mice. **A-B** The cumulative frequencies, enumeration and gMFI of IL-4 (**A**) and IL-5 (**B**) in heart to ILC2s after IL-33 stimulation for 4 hours by flow cytometric analysis. Each dot represents one mouse; different color represents different litter; error bars represent mean ± SD. *p < 0.05. Unpaired two-tailed Student's t-test (A-B).

Figure 4

Ratio and cell numbers of ILC2s in the heart tissues in 8 weeks old *Rag2*$^{-/-}$ mice. **A** Cumulative frequencies and enumeration of heart ILC2s among CD45$^+$ lymphocyte in 8 weeks old *Rag2*$^{-/-}$ mice. **B** Cumulative frequencies and enumeration of KLRG1$^-$ILC2s and KLRG1$^+$ILC2s among heart ILC2s in 8 weeks old *Rag2*$^{-/-}$ mice. **C** The gMFI of indicated surface makers in heart ILC2s (identification as CD45$^+$Lin$^-$CD127$^+$CD90.2$^+$ST2$^+$cells) and heart KLRG1$^-$ILC2s and KLRG1$^+$ ILC2s of 8 weeks old *Rag2*$^{-/-}$ mice. Each dot represents one mouse; error bars represent mean ± SD; **p < 0.01, ***p < 0.001. Two-way ANOVA followed by Dunnett's test (A-C).

Figure 5

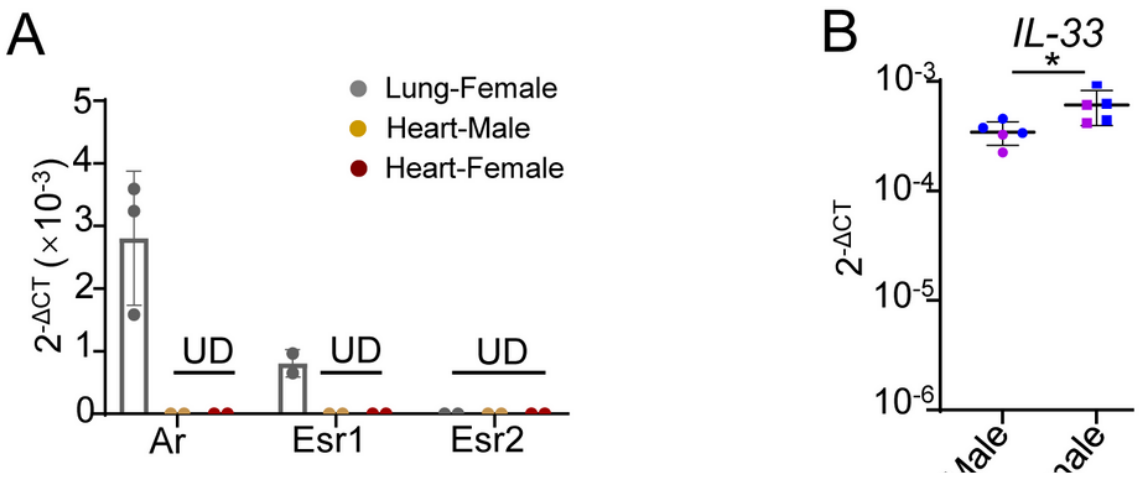

Figure 5

He levels of hormone receptors on heart ILC2s and IL-33 in the heart tissue in both male and female mice. **A** The relative mRNA expression of *Ar*, *Esr1*, and *Esr2* in both lung and heart ILC2s. **B** The relative mRNA expression of *IL-33* within the heart tissues of both male and femalemice. Each dot represents one mouse; different color represents different litter; error bars represent mean ± SD. *$p < 0.05$. Unpaired two-tailed Student's t-test (A-B).

Figure 6

NA-Seq analysis of heart lymphocytes from both male and female mice. **A** Percentage of heart ILC2s in both male and female mice. Each dot represents one mouse; error bars represent mean ± SD; *$p < 0.05$; Unpaired two-tailed Student's t-test. **B** Heat map representing the relative abundance of differentially expressed genes in heart ILC2s between male and female mice. logFC threshold was set to 0.25. **C** Pathway enrichment assay of highly expressed genes fro both male and female heart ILC2s by Gene set variation analysis (GSVA) analysis.

Supplementary Files

This is a list of supplementary files associated with this preprint. Click to download.

- 20220616Supplementary.docx